

# Histopathological Image Classification Methods and Techniques in Deep Learning Field

Sudha Rani V<sup>1</sup>, M Jogendra Kumar<sup>2</sup>

<sup>1</sup>Scholar, Department of CSE, KoneruLakshmaiah Education Foundation, AP,India

Email:suchi\_asafriend@yahoo.com

<sup>2</sup>Associate Professor, Department of CSE, KoneruLakshmaiah Education Foundation, AP, India,

Email: jogendra@kluniversity.in

## Abstract

A cancerous tumour in a woman's breast, Histopathology detects breast cancer. Histopathological images are a hotspot for medical study since they are difficult to judge manually. In addition to helping doctors identify and treat patients, this image classification can boost patient survival. This research addresses the merits and downsides of deep learning methods for histopathology imaging of breast cancer. The study's histopathology image classification and future directions are reviewed. Automatic histopathological image analysis often uses complete supervised learning where we can feed the labeled dataset to model for the classification. The research methods are frequently trust on feature extraction techniques tailored to specific challenges, such as texture, spatial, graph-based, and morphological features. Many deep learning models are also created for picture classification. There are various deep learning methods for classifying histopathology images.

**Keywords:** Histopathological image, features, deep learning, morphological features.

## I. Introduction

Cancer of the breast (BC) is the important prevalent malignant tumour in the universe of women. BC is the foremost disease in incidence rate (24.2 percent) and the mortality rate (40 percent) among women with cancer worldwide in 2018, according to the latest available figures [1]. (15 percent). It is one of the most serious health threats to female health. In developing nations, the majority of women who are diagnosed with breast cancer do not survive because the disease is identified too late. Early detection of BC can significantly reduce the mortality rate. As a result, early detection is only the way in BC prevention. Different images ( X-rays, ultra sound) imaging can be used to identify and diagnose BC [2, 3]. Imaging for cancer screening was introduced in 1973 [3]. Tissue biopsy is the most accurate means of determining whether or not cancer is present in a patient. As a result, histopathology images are the most reliable method of diagnosing practically all cancers, including breast cancer [4]. Under the supervision of pathologists, the decision of BC has clear by inspecting histological samples under magnifying glasses and performing grading and analysis of the phases. The breast cancer histopathology images will undergo through pre-processing and then the respective features are derived for classification task. Most cases segmentation will use as pre-processing method. Because most advancements in deep learning (DL) methods, detecting and classifying of BC becomes simple. It is discussed in this article how outdated classification methods for physically extracting breast

cancer histopathological image features compare to newer DL methods for automatically extracting breast cancer histopathological image features. The Fig.1 demonstrate that the brain's connections acting as a neural network to accomplish intelligence reasoning functions. An image (from an item) that can be recognized by the human brain, and that can process words (translate language), as well as other things like eating and riding a bicycle (selfintuition).

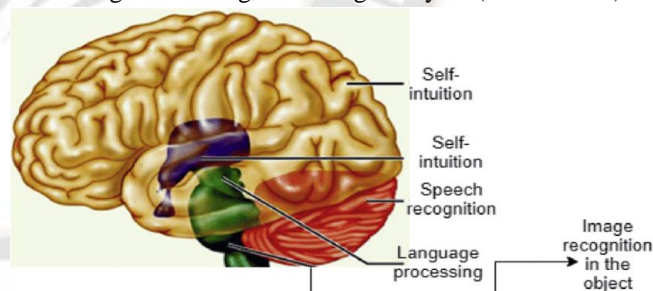


Fig.1: Human brain and individual cells.

Following that, it examines the research on merging DL and other approaches to detect and classify BC histological images. The Fig.2 show the basic work of histopathological image classification.

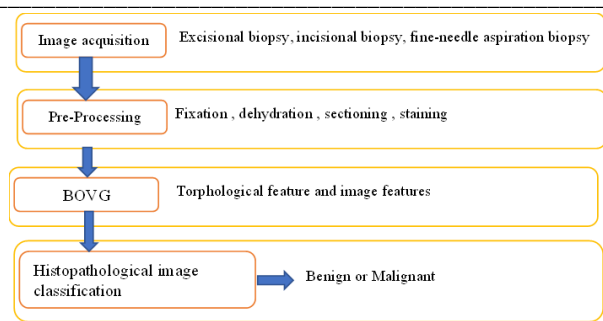


Fig.2: Basic architecture of research in histopathological image classification.

## II. Related Work

Widely utilised to extract features from images [5 -8], large artificial neural networks (LANNs) are DL models. DL models have also analysed histopathology pictures. DL models like AlexNet [9], ResNet-18 [10], and GoogleNet [11] have recently used transfer-learning to fine-tune. Much of information or datasets are required to learn and squeeze the hyper-parameters. However, most histopathology pictures are private. Working with limited data is difficult with DL. It's possible to capture some basic differences without deep characteristics.

These photos use BoVW characteristics (sparsity and high inter-class similarity). For each image in the collection, they look for visual terms that help solve the dependent class similarity problem. BoVW-based feature extraction is popular in both traditional and DL-based approaches because it captures semantic information from pre-trained DL models' feature maps. The Bag of Deep Visual Words (BoDVW) features may not operate well in other domains due to visual variations. However, DCF-BoVW [12] intended for satellite photos may not perform well with CXR images. DCF-BoVW might gather enough semantic regions from satellite photos since they are dense. However, DCF-BoVW may not capture all semantic regions in CXR pictures. VGG16 DL model (4th pooling layer) [13] avg (4th pooling layer) RAW FEATURE MAPS We use the 4th pooling layer provided by Sitaula et al. So we normalize each deep feature vector by its depth. Using the training data, we generate a codebook/dictionary. Then we use the codebook to get features for each image. L2-norm normalizes the final image representation using the bag of visual words method. Our final features use patterns extracted from training photos to discriminate sparse histopathology images.

Deep Learning (DL) revolutionizes image processing by enhancing classification and object detection. A DL model is a huge ANN fashioned after the human brain. A user-

defined DL model is one we build ourselves. Pre-trained deep learning models use huge datasets like ImageNet or Places. [15]. Unlike standard computer vision approaches like Scale Invariant Feature Transform (SIFT) [16], GIST-color [17], etc., the features collected from intermediate layers of DL models give rich semantic features to represent images. Xception [18] and VGG16 [13] utilized. A better classification model than Xception is VGG16 (87.00 percent versus 82.00 percent). This helps the VGG16 model represent and categorise CXR pictures. This led to widespread usage of pre-trained models in histopathology. SVM [19], Random Forest [20], k-nearest neighbors [21], and Naive Bayes [22] were utilized by Varshni& co. to extract features from pre-trained models such VGG16, Xception, ResNet50, DenseNet121, and DenseNet169. The DenseNet-169 model using SVM features had the greatest AUC score of 80.02 percent among all models tested. Loey et al. [23] trained Generative Adversarial Networks (GAN) on AlexNet [9], ResNet18 [10], and GoogleNet [11] to categorize histopathology pictures. (Good, Bad) A two-class issue (Benign, Malignant). For histopathology pictures, most known approaches extract high-level characteristics. They require neither too general nor too specific features. It is a hot topic in medical image processing and deep learning [24, 25]. For whole slide images (WSIs), typical machine learning and deep neural network models are difficult to train [26]. Then train a classifier with the segmented nuclei [25]. The watersheds algorithm [27] was used to refine George et al. This research extracted morphology, topology, and texture. Use these to train classifiers. They then evaluated four classifiers with 80%-85% accuracy. The above results were accepted but unstable. The model's representativeness is determined. Results are poor and unstable when using the best descriptor or combining descriptors [28]. CNNs are now being employed for visual classification [29]. As a result, CNN deep learning is difficult or impossible. A lot of detail is lost when downsizing full histopathology photos for deep learning. For this, researchers developed patch-based picture classification. They utilised AlexNet [30] and three fusion rules to categorize. Arajo et al. presented a CNN architecture [31]. Invasive images were trained to the network to classify as normal. CNN could extract picture patches to train WSIs. Hou et al (patch-level). Multiclass Logistic Regression (or Support Vector Machine) is based on Expectation Maximization (SVM). It was proposed by Alom et al. WTA was used to classify the final results [32]. Figures 3 and 4 exhibit BOVW feature extraction.

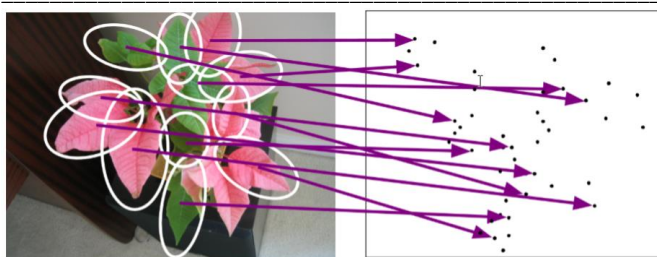


Fig.3: Bag of visual words (BOVW) feature extraction.

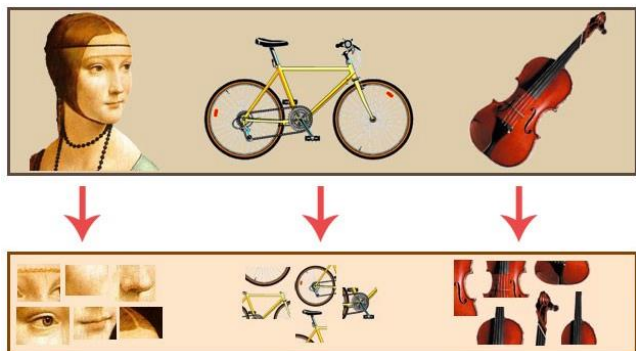


Fig.4: Sample outcome of features from the image.

Table 1: Related work and their prominent features and limitations.

|   |  |
|---|--|
| Pin Wang ,Pufei Li , Yongming Li , Jiaxin Wang , Jin Xu , “ [2021] [33] |  |
| Model Used  | Cross-domain transfer learning and multi-stage feature fusion (CD-DTFFNET)   |
| Prominent features  | <ul style="list-style-type: none"> <li>Using of multiple layers</li> <li>The features fusion and with L2 regularity are fully use the different feature scales</li> <li>Fully demonstrate cross-domain transfer learning</li> <li>The strategy of feature fusion</li> </ul>  |
| Limitations   | <ul style="list-style-type: none"> <li>Too complex in architecture</li> <li>Fusion of many features will lead to over fitting</li> </ul>   |
| Manisha Saini, Seba Susan [2020] [34]                                   |  |
| Model Used  | <ul style="list-style-type: none"> <li>Deep convolution generative Adversarial network (DCGAN)</li> </ul>  |
| Prominent features  | <ul style="list-style-type: none"> <li>Evaluated the impact of DCGAN and normalization</li> <li>It helps detect cancer cells early.</li> <li>Both negative and positive bags contain class-specific and irrelevant examples.</li> <li>The presence of irrelevant data examples and prior information on sparse relevant instances</li> </ul> |

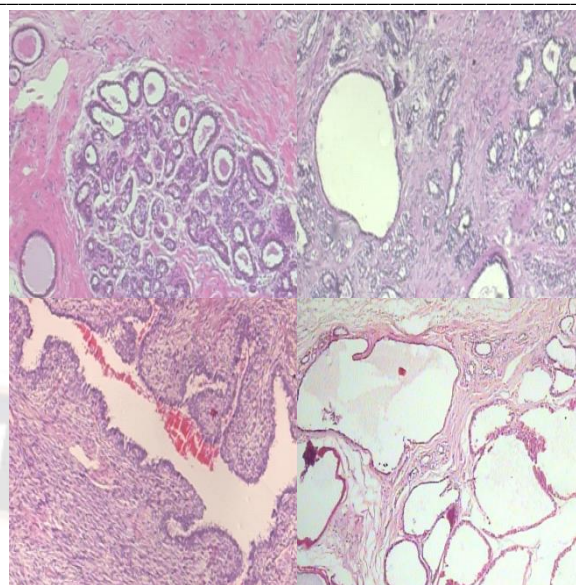
|   |  |
|---|--|
| Limitations   | <ul style="list-style-type: none"> <li>DCGAN relies on minority class samples to improve classifier performance.</li> <li>DCGAN training distribution won't generalise well in scenarios with few minority samples, resulting in sub-optimal performance.</li> </ul>   |
| Trung Vu, RavivRaich, UK Arvind Rao [2020] [35]   |  |
| Model Used  | <ul style="list-style-type: none"> <li>Novel symmetric multiple instance learning (MIL) framework</li> </ul>   |
| Prominent features  | <ul style="list-style-type: none"> <li>Good in accuracy</li> </ul>   |
| Limitations   | <ul style="list-style-type: none"> <li>It won't give efficient results for all kind of images</li> <li>Not used any pre-trained models</li> </ul>  |
| Yusuf Celik ,MuhammedTalo , OzalYildirim , Murat Karabatak , U Rajendra Acharya [2020] [36] |  |
| Model Used  | Deep transfer learning technique   |
| Prominent features  | <ul style="list-style-type: none"> <li>A method for automatic IDC</li> <li>Only the last layers of the models are trained, and the test participants are not used in the training set.</li> </ul>  |
| Limitations   | <ul style="list-style-type: none"> <li>It is used for scanning image dataset</li> <li>It is considered for small dataset</li> </ul>  |
| Said Boumaraf ,Xiabi Liu , ZhongshuZheng, Xiaohong Ma , ChokriFerkous [2021] [37]           |  |
| Model Used  | <ul style="list-style-type: none"> <li>Deep neural network ResNet-18</li> <li>Transfer learning method is used.</li> <li>11 architectures</li> </ul>   |
| Prominent features  | <ul style="list-style-type: none"> <li>Using GCN- and three-fold data augmentation on train set, the suggested model is more adaptable.</li> <li>The obtained results proved the proposed approach's effectiveness, with accuracy between 98.08% and 99.25%</li> </ul> |
| Limitations   | <ul style="list-style-type: none"> <li>Color influences breast histopathological image classification.</li> <li>Combine CNN intrinsic features with handcrafted features to improve eight-class classification.</li> </ul>   |
| Xi Wang , Hao Chen, Huangjing Lin, Qi Dou, Pheng-Ann Heng [2020] [38]                       |  |

|   |  |
|---|--|
| Model Used  | Fully convolutional network (FCN)  |
| Prominent features  | <ul style="list-style-type: none"> <li>• Patch-based FCN retrieves discriminative</li> <li>• We built the largest fine-grained lung cancer. Then we tested our technique on a public lung cancer WSI dataset. TCGA WSIs dataset (The Cancer Genome Atlas)</li> </ul> |
| Limitations   | <ul style="list-style-type: none"> <li>• Its too complex in architecture</li> </ul>  |
| Wang, Qi Song, Yongming Li, ShanshanLv, Jiaxin Wang, LinyuLi, HeHua Zhang [2020] [39] |  |
| Model used  | <ul style="list-style-type: none"> <li>• Double deep transfer learning (D2TL) and interactive cross-task extreme learning machine (ICELM)</li> </ul>   |
|   | <ul style="list-style-type: none"> <li>• Deep and double-step deep transfer learning extract high-level features.</li> <li>• The proposed ICELM uses both TL and DSTL features.</li> <li>• Both source and target losses are considered</li> </ul>                   |
| Limitations   | <ul style="list-style-type: none"> <li>• Need of coherent to reduce computational complexity</li> <li>• To reduce complexity in training time and computation time, need modifications in CNN</li> </ul>   |

The Table 1 clearly exhibits the different author’s contributions and respective pros and cons.

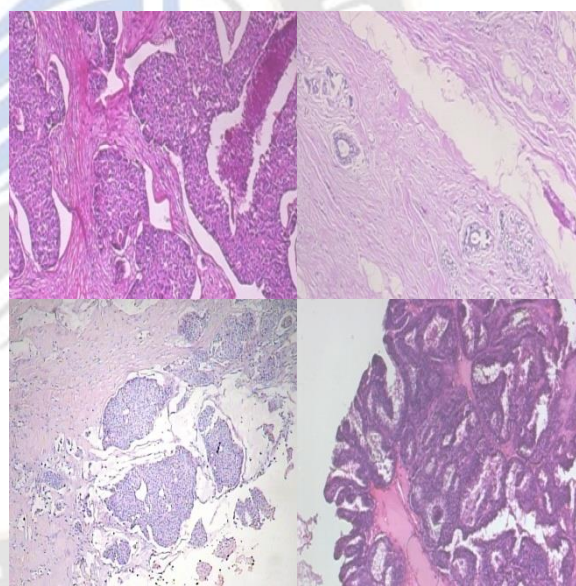
### 1.1 Dataset

BreaKH is the most recent public breast cancer histopathological imaging collection, from 2014. The P&D Laboratory (Brazil) invited breast cancer patients to participate [40]. The study was authorized by the IRB and all patients gave written informed permission. Anonymization was used for all data. Hematoxylin and eosin was used to stain breast tissue biopsy slides (H&E). The samples were obtained via surgical open biopsy (SOB), processed for histological study, and labelled by P&D pathologists. Each instance was diagnosed by a pathologist and immunohistochemically verified [27]. Currently, BreaKH contains 7909 histopathology biopsy images from 82 individuals. A total of four magnification factors were used to gather images in three-channel RGB colour space (40X, 100X, 200X, and 400X). Figures 5 and 6 show 40X magnified samples of eight sub-categories of breast cancers.



(a) Adenosis (b) Fibroadenoma (c) Phyllodes Tumor (d) Tubular

Fig.5: Sample images of Benign category (Adenoma).



(e) Ductal (b) Lobular (c) Mucinous (d) Papillary

Fig.6: Sample images of malignant category.

Table 2: Description of dataset in terms of categories and number of patients.

| Main category | Sub-Categories | Magnifications |     |     |     | Patients |
|---------------|----------------|----------------|-----|-----|-----|----------|
|               |                | 11x            | 11x | 11x | 10x |          |
| Benign        | Adenosis       | 6              | 5   | 3   | 8   | 6        |
|               |                | 25             | 26  | 26  | 23  |          |
|               | Fibroadenom    | 5              | 2   | 6   | 9   | 12       |
|               |                | 15             | 15  | 14  | 13  | 5        |

|           |                     |    |    |    |    |    |
|-----------|---------------------|----|----|----|----|----|
|           | a                   | 1  | 2  | 2  | 2  |    |
|           | Phyllodes Tumor     | 11 | 12 | 11 | 11 | 9  |
|           | Tubular Adenoma     | 86 | 90 | 89 | 79 | 40 |
| Malignant | Ductal Carcinoma    | 15 | 17 | 16 | 13 | 7  |
|           | Lobular Carcinoma   | 20 | 22 | 19 | 17 | 11 |
|           | Mucinous Carcinoma  | 14 | 14 | 13 | 14 | 8  |
|           | Papillary Carcinoma | 11 | 11 | 11 | 10 | 6  |

Fig.4 shows the traditional classification of breast cancer histopathological images. Main module is feature extraction. Breast cancer histopathological images were classified using some of the same image feature extraction algorithms.

### 2.1. Feature extraction

A typical image aspect is colour distribution. This has been examined widely. LBP is an image texture operator. Ojala proposed it first [41]. In 2002, Ojala wrote about the LBP operator on PAMI [42]. Gui et al [43] presented a CLBP operator distinct from the LBP operator. A texture categorization tool with three descriptors: CLBP-M, CLBP-S, and CLBP-C. Classify breast cancer photos using derived texture attributes. The categorization of early BC histopathology images has advanced significantly. Using adaptive threshold technology and Gaussian mixture clustering, 500 BC histopathology images are 92-98% accurate. Filipczuk et al. [44] suggested using fine-needle biopsy histopathological image analysis to detect breast cancer. Four classifiers trained with 25-dimensional feature vectors accurately classified 737 photos. On 92 images, George et al. [45] obtained 76-94 percent accuracy using fuzzy C-means clustering and Otsu threshold approach to eliminate noise. Wang et al. [46] proposed assessing breast cancer histopathology imagesutilising multi-scale regional growth. The approach paired with wavelet transform classifies 68 BC histopathology images with 96.19% accuracy. Osareh et al. [47] employed KNN, PNN, and SVM to diagnose BC. Deep learning has absorbed decades of neuroscience, statistics, and applied mathematics knowledge. Larger data sets and new training deep networks have enhanced computer performance significantly. Images are classified and recognized. Fabio et al. [48] used AlexNet to categorize fusion blocks on the BreakHis dataset. In this process, photos are automatically extracted and classified, increasing accuracy by 6%. BreakHis data analysis Aim for a magnification-independent algorithm. To classify images

without magnification, Bayramoglu et al. [49] suggested a dual CNN classification technique. Using deep learning, predict malignant tumour magnification and classify BC histopathology images. The accuracy is 83%. Song et al. [50] increased the accuracy of the BreakHis dataset classification model by combining convolutional neural networks and Fisher vectors. Their shortcomings are their sudden visual components and dimensionality. Song et al. [51] developed a volume-based supervised embedding method. Convolutional neural networks have been used in image classification and recognition, object recognition, natural language processing, and more. Recent research reveals that deep learning can enhance classification accuracy for breast cancer histopathology images. Insufficient training data restricts deep learning network performance. So scholars use numerous technologies to answer the problem. Applying previously obtained knowledge to new challenges can improve results. It's called transfer learning. Spanhol [52] used transfer learning to extract depth information from breast cancer histopathology images and input them to the classifier. This technique addresses issues such as more training time and insufficient data.

### III. Performance parameters

F1 score is the weighted normal of Precision and Recall. Hence, this score considers both false positive examples and false negative examples. The precision is determined utilizing condition (7).

The performance metrics are: sensitivity (St), specificity (Sp), precision (Pr), F-score (FS) and Accuracy (Ac). These measures are computed from confusion matrix and respective Eqns. are written below:

$$Accuracy = \frac{True\ Positive + True\ Negative}{(True\ Positive + false\ negative) + (false\ Positive + True\ Negative)} \quad (1)$$

$$Se = \frac{True\ Positive}{True\ Positive + False\ Negative} \quad (2)$$

$$Sp = \frac{True\ Negative}{True\ Negative + False\ Positive} \quad (3)$$

$$Pr = \frac{True\ Positive}{True\ Positive + FP} \quad (4)$$

$$F_{Score} = \frac{2 * True\ Positive}{2 * True\ Positive + False\ Positive + False\ Negative} \quad (5)$$

Where True positive (TP) reflects the classification of positives, such as cancer, and true negative (TN) represents the classification of negatives, such as infection. Furthermore, false positive (FP) reflects samples that have been erroneously identified, and false negative (FN) indicates cancer images that have been labelled as normal.

We compared our method to R-ResNet [53], DTL [54], and D2TL ICELM [55]. (Interactive cross-task extreme learning machine) To examine the effectiveness of cross-domain transfer learning, Cd-DTL is compared to DTL and BKTL. It displays the efficacy of feature fusion between different tiers. To show feature fusion, the proposed Cd-dtffNet is compared to Cd-DTL and D2TL ICELM [73]. Table 3 compares the accuracy, sensitivity, and specificity of various models for Normal versus Malignant.

Table 3: Comparison of different methods of breast cancer classification in terms of accuracy (Acc(%), sensitivity (Sen(%)) and Specificity (Spe (%)).

| Type                 | Method      | Accuracy     | Sensitivity  | Specificity  |
|----------------------|-------------|--------------|--------------|--------------|
| Normal VS Malignant  | R:ResNet    | 79.64 ± 2.98 | 58.57 ± 9.44 | 85.07 ± 7.42 |
|                      | D2TL_ICE LM | 98.18 ± 0.05 | 92.00 ± 0.96 | 100.00 ± 0   |
|                      | DTL         | 95.45 ± 2.87 | 97.14 ± 5.72 | 94.67 ± 4.99 |
|                      | DTL-Fuse    | 97.27 ± 2.23 | 97.14 ± 5.72 | 97.33 ± 3.27 |
|                      | BKTL        | 84.23±2.22   | 74.23±2.22   | 84.23±2.22   |
|                      | BKTL-Fuse   | 90.88 ± 3.23 | 87.44 ± 4.28 | 78.57 ± 5.64 |
| Normal VS Uninvolved | R-ResNet    | 79.13 ± 4.08 | 90.00 ± 9.00 | 77.54 ± 5.38 |
|                      | D2TL_ICE LM | 96.96 ± 0.08 | 94.00 ± 1.64 | 97.58 ± 0.06 |
|                      | DTL         | 95.51 ± 1.13 | 87.59 ± 2.68 | 97.78 ± 1.81 |
|                      | DTL-Fuse    | 96.21 ± 1.62 | 94.82 ± 1.82 | 95.00 ± 6.12 |
|                      | BKTL        | 86.90 ± 2.40 | 75.12 ± 8.52 | 94.44 ± 4.85 |
|                      | BKTL-Fuse   | 94.45 ± 2.20 | 93.60 ± 7.22 | 94.44 ± 2.48 |
| Normal VS Malignant  | R-ResNet    | 81.48 ± 2.55 | 92.72 ± 1.29 | 72.56 ± 2.21 |
|                      | D2TL_ICE    | 96.67 ±      | 91.82 ±      | 100.00 ±     |

| t +        | LM        | 0.04         | 0.24         | 0            |
|------------|-----------|--------------|--------------|--------------|
| Uninvolved | DTL       | 95.72 ± 1.78 | 97.33 ± 3.27 | 94.82 ± 3.78 |
|            | DTL-Fuse  | 96.87 ± 1.38 | 97.71 ± 2.86 | 96.30 ± 2.34 |
|            | BKTL      | 90.05 ± 2.27 | 93.33 ± 2.91 | 95.44 ± 3.66 |
|            | BKTL-Fuse | 95.97 ± 2.27 | 94.85 ± 3.8  | 99.22 ± 4.20 |

#### IV. Conclusions

The following are the findings of this study on the classification of breast cancer histopathology images: Using classic machine learning approaches for histopathological image classification in breast cancer detection requires pathologists with professional clinical expertise, and the feature extraction procedure takes a long time and energy. The typical use of machine learning for histopathological image categorization in breast cancer detection is seriously harmed. Deep learning can automatically learn features from vast numbers of pictures, reducing the complexities and restrictions of older methods. The paucity of publicly available data sets has impeded the medical image sector's growth. Transfer learning can help resolve this issue, but it is not adequate. There should be more research into using Generative Adversarial Networks to analyse histological images of breast cancer. Because diverse research uses various image data, it's difficult to relate the results of different algorithm settings. In order to improve the science of automatic breast cancer image classification, a large public breast cancer histopathology image database is required. Only accuracy is not evaluation indicator and will not accurately depict an algorithm's performance objectively. The F1 value and the Area under the Curve (AUC) are two measures that can be used to compare an algorithm's performance.

#### References

- [1]. F. Bray, J. Ferlay, I. Soerjomataram, R.L. Siegel, L.A. Torre, A. Jemal, and Global cancer statistics 2018: GLOBOCAN estimates of incidence and mortality worldwide for 36 cancers in 185 countries. Bray F, Ferlay J, Soerjomataram I, Siegel RL, Torre LA, Jemal A. Global cancer statistics 2018: GLOBOCAN estimates of incidence and mortality, CA. Cancer J. Clin. 68 (2018) 394–424. doi:10.3322/caac.21492
- [2]. R.L. Siegel, K.D. Miller, A. Jemal, Cancer statistics, 2016. - PubMed - NCBI, CA. Cancer J. Clin. 66 (2016) 7–30. doi:10.3322/caac.21332
- [3]. C.E. DeSantis, S.A. Fedewa, A. Goding Sauer, J.L. Kramer, R.A. Smith, A. Jemal, Breast cancer statistics,

- 2015: Convergence of incidence rates between black and white women, *CA. Cancer J. Clin.* 66 (2016) 31–42. doi:10.3322/caac.21320
- [4]. N. Stathonikos, M. Veta, A. Huisman, P. van Diest, Going fully digital: Perspective of a Dutch academic pathology lab, *J. Pathol. Inform.* 4 (2013) 15. doi:10.4103/2153-3539.114206
- [5]. Sandeep Pande and Manna Sheela Rani Chetty, "Analysis of Capsule Network (Capsnet) Architectures and Applications", *Journal of Advanced Research in Dynamical and Control Systems*, Vol. 10, No. 10, pp. 2765-2771, 2018.
- [6]. Sandeep Pande and Manna Sheela Rani Chetty, "Bezier Curve Based Medicinal Leaf Classification using Capsule Network", *International Journal of Advanced Trends in Computer Science and Engineering*, Vol. 8, No. 6, pp. 2735-2742, 2019.
- [7]. Pande S.D., Chetty M.S.R. (2021) Fast Medicinal Leaf Retrieval Using CapsNet. In: Bhattacharyya S., Nayak J., Prakash K.B., Naik B., Abraham A. (eds) *International Conference on Intelligent and Smart Computing in Data Analytics. Advances in Intelligent Systems and Computing*, vol 1312.
- [8]. Sandeep Dwarkanath Pande, Pramod Pandurang Jadhav, Rahul Joshi, Amol Dattatray Sawant, Vaibhav Muddebhalkar, Suresh Rathod, Madhuri Navnath Gurav, Soumitra Das, "Digitization of handwritten Devanagari text using CNN transfer learning – A better customer service support", *Neuroscience Informatics*, Volume 2, Issue 3, 2022.
- [9]. AA. Krizhevsky, I. Sutskever, and G. E. Hinton, "ImageNet classification with deep convolutional neural networks," in *Proc. Adv. Neural Inf. Process. Syst.*, 2012, pp. 1097–1105.
- [10]. Wang, Fei, Mengqing Jiang, Chen Qian, Shuo Yang, Cheng Li, Honggang Zhang, Xiaogang Wang, and Xiaoou Tang. "Residual attention network for image classification." In *Proceedings of the IEEE Conference on Computer Vision and Pattern Recognition*, pp. 3156-3164. 2017.
- [11]. C. Szegedy et al., "Going deeper with convolutions," in *Proc. IEEE Conf. Comput. Vis. Pattern Recognit.*, 2015, pp. 1–9.
- [12]. Wan J, Yilmaz A, Yan L. Dcf-bow: Build match graph using bag of deep convolutional features for structure from motion. *IEEE Geosci Remote Sens Lett* 2018;15(12):1847–51.
- [13]. Simonyan K, Zisserman A. Very deep convolutional networks for large-scale image recognition. *arXiv preprint arXiv:14091556* (2014)
- [14]. Sitaula C, Hossain M. Attention-based vgg-16 model for covid-19 chest x-ray image classification. *ApplIntell* 2020. <https://doi.org/10.1007/s10489-020-02055-x>
- [15]. Zhou B, Khosla A, Lapedriza A, Torralba A, Oliva A. Places: an image database for deep scene understanding. *arXiv preprint arXiv:161002055* (2016).
- [16]. Lowe DG. Distinctive image features from scale-invariant keypoints. *Int J Comput Vis.* 2004;60(2):91–110.
- [17]. Oliva A, Torralba A. Modeling the shape of the scene: a holistic representation of the spatial envelope. *Int J Comput Vis.* 2001;42(3):145–75.
- [18]. Chollet F. Xception: Deep learning with depthwise separable convolutions. In: *Proc. IEEE Conf. Comput. Vis. Pattern Recognit.*, pp 1251–1258 (2017)
- [19]. Hearst MA. Support vector machines. *IEEE Intell Syst.* 1998;13(4):18–28.
- [20]. Breiman L. Random forests. *Mach Learn.* 2001;45(1):5–32.
- [21]. Pande, Sandeep Dwarkanath et al. 'Shape and Textural Based Image Retrieval Using K-NN Classifier', *Journal of Intelligent & Fuzzy Systems*, vol. 43, no. 4, pp. 4757-4768, 2022.
- [22]. Lewis DD. Naive (bayes) at forty: The independence assumption in information retrieval. In: *Proc. European Conference on Machine Learning*, pp 4–15 (1998)
- [23]. Loey M, Smarandache F, Khalifa M. Within the lack of chest covid-19 x-ray dataset: a novel detection model based on gan and deep transfer learning. *Symmetry.* 2020;12(4):651.
- [24]. J. Xie, R. Liu, J. Luttrell, and C. Zhang, "Deep learning based analysis of histopathological images of breast cancer," *Frontiers Genet.*, vol. 10, p. 80, Feb. 2019.
- [25]. C. Kaushal, S. Bhat, D. Koundal, and A. Singla, "Recent trends in computer assisted diagnosis (CAD) system for breast cancer diagnosis using histopathological images," *IRBM*, vol. 40, no. 4, pp. 211–227, Aug. 2019.
- [26]. A. Das, M. S. Nair, and S. D. Peter, "Computer-aided histopathological image analysis techniques for automated nuclear atypia scoring of breast cancer: A review," *J. Digit. Imag.*, pp. 1–31, Jan. 2020, doi: 10.1007/s10278-019-00295-z.
- [27]. L. Vincent and P. Soille, "Watersheds in digital spaces: An efficient algorithm based on immersion simulations," *IEEE Trans. Pattern Anal. Mach. Intell.*, vol. 13, no. 6, pp. 583–598, Jun. 1991.
- [28]. Y. Benhammou, B. Achchab, F. Herrera, and S. Tabik, "BreakHis based breast cancer automatic diagnosis using deep learning: Taxonomy, survey and insights," *Neurocomputing*, vol. 375, pp. 9–24, Jan. 2020
- [29]. M. Hammad, P. P<sup>a</sup>awiak, K. Wang, and U. R. Acharya, "ResNet\_Attention model for human authentication using ECG signals," *Expert Syst.*, p. e12547, Mar. 2020, doi: 10.1111/exsy.12547
- [30]. Y. Lecun, L. Bottou, Y. Bengio, and P. Haffner, "Gradient-based learning applied to document recognition," *Proc. IEEE*, vol. 86, no. 11, pp. 2278–2324, Nov. 1998.
- [31]. T. Araújo, G. Aresta, E. Castro, J. Rouco, P. Aguiar, C. Eloy, A. Polónia, and A. Campilho, "Classification of breast cancer histology images using convolutional neural networks," *PLoS ONE*, vol. 12, no. 6, Jun. 2017, Art. no. e0177544.

- [32]. J. Lazzaro, S. Ryckebusch, M. A. Mahowald, and C. A. Mead, "Winnertake- all networks of O (n) complexity," in Proc. Adv. Neural Inf. Process. Syst., 1989, pp. 703-711.
- [33]. Pin Wang, Pufei Li, Yongming Li, Jiaxin Wang, Jin Xu, Histopathological image classification based on cross-domain deep transferred feature fusion, Biomedical Signal Processing and Control 68 (2021) 102705
- [34]. Saini, Manisha, and Seba Susan. "Deep transfer with minority data augmentation for imbalanced breast cancer dataset." Applied Soft Computing 97 (2020): 106759.
- [35]. Trung Vu, Raviv Raich, UK Arvind Rao, A Novel Attribute-Based Symmetric Multiple Instance Learning for Histopathological Image Analysis, IEEE transactions on medical imaging, VOL. 39, NO. 10, OCTOBER 2020
- [36]. Yusuf Celik, Muhammed Talo, Ozal Yildirim, Murat Karabatak, U Rajendra Acharya, Automated Invasive Ductal Carcinoma Detection Based Using Deep Transfer Learning with Whole-Slide Images, Pattern Recognition Letters (2020), <https://doi.org/10.1016/j.patrec.2020.03.011>
- [37]. Said Boumaraf, Xiabi Liu, A new transfer learning based approach to magnification dependent and independent classification of breast cancer in histopathological images, September 2020 Biomedical Signal Processing and Control 63 (January 2021):1746-8094
- [38]. Xi Wang, Hao Chen, Qi Dou, Efstratios Tsougenis, Qitao Huang, Muyan Cai, and Pheng-Ann Heng, Weakly Supervised Deep Learning for Whole Slide Lung Cancer Image Analysis, IEEE Transactions On Cybernetics, Vol. 50, NO. 9, SEPTEMBER 2020
- [39]. features Pin Wang, Qi Song, Yongming Lia, Shanshan Lva, Jiaxin Wang, Linyu Lia, He Hua Zhang, Cross-task extreme learning machine for breast cancer image classification with deep convolutional features, Biomedical Signal Processing and Control 63 (2021) 102192
- [40]. F. A. Spanhol, L. S. Oliveira, C. Petitjean, and L. Heutte, "A dataset for breast cancer histopathological image classification," IEEE Trans. Biomed. Eng., vol. 63, no. 7, pp. 1455-1462, Jul. 2016.
- [41]. Ojala T, Pietikäinen M, Harwood D 1996 Pattern. Rec. 29 51-59
- [42]. Ojala T, Pietikainen M, Maenpaa T 2002 IEEE Trans. on Pattern Anal. and Mach Intell. 24 971- 987
- [43]. Guo Z, Zhang L, Zhang D 2010 IEEE Trans. on Image Proc. 19 1657-1663.
- [44]. Filipczuk P, Fevens T, Krzyak A 2013 IEEE Trans. on Med. Imaging 32 2169-2178.
- [45]. George Y M, Zayed H H, Roushdy M I 2013 IEEE Sys. J. 8 949-964.
- [46]. Wang P, Hu X, Li Y 2016 Signal Processing 122 pp 1-13
- [47]. Osareh A, Shadgar B 2010 5th Int. Symp. on Health Info. and Bio. 114-120.
- [48]. Spanhol F A, Oliveira L S, Petitjean C 2016 IJCNN. 2560-2567.
- [49]. Bayramoglu N, Kannala J, Heikkilä J 2016 ICPR. 2440-2445
- [50]. Song Y, Zou J J, Chang H 2017 ISBI. 600-603
- [51]. Song Y, Chang H, Huang H 2017 Int. Conf. on Med. Image Comp. and Computer-Assisted Interv. 99-106.
- [52]. Spanhol F A, Oliveira L S, Cavalin P R 2017 IEEE Int. Conf. on SMC 1868-1873.
- [53]. S. Pouyanfar, S.C. Chen, M.L. Shyu, An efficient deep residual-inception network for multimedia classification, IEEE International Conference on Multimedia and Expo (2017) 373-378, <http://dx.doi.org/10.1109/ICME.2017.8019447>.
- [54]. M. Oquab, L. Bottou, I. Laptev, et al., Learning and Transferring Mid-level Image Representations Using Convolutional Neural Networks[C]// Computer Vision and Pattern Recognition, 2014, pp. 1717-1724, <http://dx.doi.org/10.1109/CVPR.2014.222>.
- [55]. G.B. Huang, H. Zhou, X. Ding, et al., Extreme learning machine for regression and multiclass classification, IEEE Trans. Syst. Man Cybern. B Cybern. 42 (2)(2012) 513-529, <http://dx.doi.org/10.1109/tsmcb.2011.2168604>.